J. Fluid Mech. (1994), *vol.* 273, *pp.* 361–374

On a nonlinear thermocapillary effect in thin liquid layers

By ALEXANDER ORON[1] AND PHILIP ROSENAU[1,2]

[1] Faculty of Mechanical Engineering and Center for Research in Nonlinear Phenomena, Technion–Israel Institute of Technology, Haifa 32000, Israel

[2] Center for Nonlinear Studies, MS-B258, Los Alamos National Laboratory, Los Alamos, NM 87545, USA

(Received 7 June 1993 and in revised form 3 February 1994)

Dilute aqueous solutions of long alcohol chains were recently found to cause a *quadratic* dependence of surface tension on the temperature without affecting other bulk properties of the liquid: $\sigma = \sigma_0 + \alpha_Q (T - T_0)^2$, $\alpha_Q > 0$. The impact of such Marangoni instability on the behaviour of a thin liquid layer is studied in this work. We derive an equation describing a nonlinear spatiotemporal evolution of a thin film. The behaviour of the perturbed film in the absence of gravity, critically depends on whether the temperature T_0, yielding a minimal surface tension, is attained on the surface of the film. When this is the case, a qualitatively new behaviour is observed: perturbations of the film interface may evolve into continuous steady patterns that do not rupture. Otherwise, the observed patterns due to the linear and quadratic Marangoni effects are qualitatively similar and result in the rupture of the film into separate drops.

1. Introduction

A liquid film at rest on a horizontal plane, exposed at its free surface to the ambient gas, when subjected to a transverse temperature gradient, may undergo a transition into a convective motion. In the absence of gravity, the thermocapillarity (also known as the Marangoni effect), induces destabilizing surface shear stresses which can overcome the stabilizing action of fluid viscosity and thermal conductivity.

In almost all studied cases of two fluids (liquid–liquid or liquid–gas) in contact (Pearson 1958; Davis 1987), the dependence of surface tension on the temperature was approximated by a linearly decreasing function of the temperature:

$$\sigma = \sigma_0 - \alpha_L (T - T_0), \quad \alpha_L > 0, \tag{1}$$

where σ_0 is the surface tension at the reference temperature T_0 and α_L is the surface tension gradient measured in units of $\mathrm{N\,(m\,K)^{-1}}$. This type of variation has a considerable empirical support and is in tandem with linear transport theory. It predicts surface tractions to be directed from the locally hottest spot on the free surface of the film toward the locally coldest one. This is the essence of the linear Marangoni effect (LM). However, in principle, nothing precludes a nonlinear temperature dependence, and, in fact, other types of surface-tension dependence on temperature have recently been measured (Guyon & Pantaloni 1980; Legros, Limbourg-Fontaine & Petre 1984). Binary metallic alloys were found to exhibit a monotonically increasing – rather than decreasing – linear dependence (Guyon & Pantaloni 1980), $\alpha_L < 0$. It was also found (Legros *et al.* 1984) that dilute aqueous solutions of long alcohol chains show a *non-monotone* dependence of surface tension on the temperature. In such

solution, bulk properties like those of density and viscosity do not change – the surface tension of the dilute aqueous solution was found to have a well-pronounced minimum that can be approximated fairly well by the quadratic expression

$$\sigma = \sigma_0 + \alpha_Q (T - T_0)^2, \quad \alpha_Q > 0, \tag{2}$$

where T_0 is the temperature at which surface tension attains its minimum value, σ_0, and α_Q is the value associated with the curvature of the surface-tension variation with temperature, measured in units of $\mathrm{N\,m^{-1}\,K^{-2}}$. While some preliminary experiments and analytical studies were recently reported (Legros 1986; Limbourg & Georis 1989; Cloot & Lebon 1986; Gupalo & Ryazantsev 1989; Gupalo, Ryazantsev & Skvortsova 1990), the nonlinear dependence of surface tension on the temperature requires a full nonlinear treatment and is still very much a terra incognita. Linear stability analysis has revealed (Cloot & Lebon 1986) that in the case of large Prandtl number, steady patterns in the form of rolls, rectangles and hexagons are admissible and the latter planform is stable. Several self-similar solutions were numerically calculated for the temperature gradient imposed along the free surface of the film (Gupalo & Ryazantsev 1989; Gupalo *et al.* 1990).

To understand the implication of a quadratic surface-tension dependence (2) on the temperature, a consistent full nonlinear study is undertaken in the present work. We shall formulate, derive and then follow the nonlinear spatiotemporal evolution of a thin liquid layer due to a nonlinear thermocapillary effect. In a natural extension of the linear Marangoni (LM) case, we shall refer to this mechanism as to the quadratic Marangoni (QM) instability.

The essence of our studies can be described as follows; we show that the QM instability enables an existence of new stable steady states which in variance with the conventional Marangoni induced patterns, are continuous and *do not rupture*. These states are possible when temperature ranges of films centre around the minimum peak of surface tension where the quadratic effect is most pronounced. On the monotone parts of $\sigma(T)$, the surface-tension temperature curve, the observed patterns are similar to the LM induced flow. Nevertheless, the quadratic effect introduces a change in stability threshold. Thus the actual physical parameters which cause a specific pattern to emerge do change. We will show instances where the stability properties of the QM- and LM-induced flows are related, which is to say that QM unstable(stable) states are either LM unstable(stable) or to the contrary, opposite relations follow. In other parameter ranges definite relations cannot be inferred and stability or instability of LM flow cannot be related to QM instability.

The possibility of endowing surface tension with a quadratic temperature dependence enables one to envisage potential applications where it might be an advantage to induce such a dependence artificially. Positioning of the temperature peak at a specific temperature may enable us to assure or to preclude the formation of a specific pattern.

In the next section we formulate and derive our model. In §3 we present numerical results of a two-dimensional version of our problem. The summary follows in §4.

2. Formulation of the model

Consider a thin incompressible liquid layer lying on a horizontal plane held at the uniform temperature T_1, with free surface open to ambient air (at temperature T_2 and pressure p_a). Surface tension σ is assumed to have a quadratic dependence on the temperature T (equation (2)). The thermal diffusivity, η, viscosity, μ, and density, ρ, of the fluid are assumed to be temperature-independent.

We begin with equations governing the incompressible flow

$$\boldsymbol{v}_t+(\boldsymbol{v}\cdot\boldsymbol{\nabla})\boldsymbol{v}=-\frac{1}{\rho}\boldsymbol{\nabla}p+\boldsymbol{g}+\frac{\mu}{\rho}\nabla^2\boldsymbol{v}, \tag{3}$$

$$\boldsymbol{\nabla}\cdot\boldsymbol{v}=0, \quad T_t+\boldsymbol{v}\cdot\boldsymbol{\nabla}T=\eta\nabla^2T. \tag{4a, b}$$

The notation is standard: $\boldsymbol{v}=\{v_1,v_2,v_3\}$ and p are the fluid velocity and the pressure, respectively.

The relevant boundary conditions are:

(i) On the plane $x_3=0$ a no-slip condition is imposed on the velocity, and a uniform temperature T_1 is specified:

$$\boldsymbol{v}=0, \quad T=T_1. \tag{5}$$

(ii) On the free film surface located at $x_3=H(x_1,x_2,t)$, we require

(*a*) balance of stresses

$$-(p-p_a)\boldsymbol{n}+2\mu\boldsymbol{D}\cdot\boldsymbol{n}=2\sigma K\boldsymbol{n}+\nabla_s\sigma, \tag{6}$$

(*b*) convective heat transfer condition:

$$\frac{\partial T}{\partial n}+q(T-T_2)=0. \tag{7}$$

The location of the interface is determined via the kinematic condition:

$$\frac{\partial H}{\partial t}+\boldsymbol{v}\cdot\boldsymbol{\nabla}H^*=0. \tag{8}$$

In equations (6) and (7), $\boldsymbol{D}$ is the stress tensor, K is the mean interfacial curvature, q is the ratio between the heat transfer rates via convection and the conduction, $\boldsymbol{n}$ is the normal unit vector, ∇_s is the surface gradient at the interface, and $H^*=-x_3+H(x_1,x_2,t)$.

We introduce the longitudinal (transverse) lengthscale $l(a)$ and a characteristic velocity U (to be determined in a moment) and define the following dimensionless quantities:

$$\left.\begin{aligned}&\epsilon\equiv\frac{a}{l}, \quad \tau^*=\frac{Ut}{l}, \quad (x,y,z)=\frac{(x_1,x_2,\epsilon^{-1}x_3)}{l},\\ &P=(p-p_a)\frac{a^2}{Ul\mu}, \quad h=\frac{H}{a}, \quad (u,v,w)=\frac{(v_1,v_2,\epsilon^{-1}v_3)}{U},\end{aligned}\right\} \tag{9a}$$

a being the mean film thickness and

$$\theta=\frac{T-T_-}{T_+-T_-}. \tag{9b}$$

T_- and T_+ are, respectively, the lowest and highest temperatures at the film boundaries, $T_+=\max(T_1,T_2)$, $T_-=\min(T_1,T_2)$.

The derivation is based on scaling (9) and with $\epsilon\ll1$ is essentially a thin film approximation and thus follows closely the method used in (Burelbach, Bankoff & Davis 1988; Oron & Rosenau 1992). The reference velocity is chosen as $U=\epsilon U_0$ with U_0 defined via

$$U_0=\frac{\alpha_Q}{2\mu}(T_+-T_-)^2\equiv Ma_Q\frac{\eta}{a}, \tag{10}$$

where Ma_Q is a nonlinear Marangoni number defined for the QM to be

$$Ma_Q = \frac{\alpha_Q}{2\mu\eta}(T_+ - T_-)^2 a.$$

The other dimensionless quantities used are similar to the ones used in (Oron & Rosenau 1992), the Reynolds, Prandtl, Biot, Weber and Bond numbers are introduced as follows: let $\nu = \mu/\rho$ be the kinematic viscosity of the fluid, then we define $Re = U_0 a/\nu$, $Pr = \nu/\eta$, $B = aq$, $S = \sigma_0/(\mu U_0)$, $G = ga^2/(3U_0\nu)$. Note that in our derivation $Re = O(1)$, $Pr = O(1)$, $B = O(1)$, $G = O(1)$, and $S = s\epsilon^{-2}$, with $s = O(1)$. Therefore for the Marangoni number we have $Ma_Q = Re\,Pr = O(1)$.

Applying the thin-film approximation (9)–(10) to (3)–(8) we obtain for the pressure, temperature and velocity components of the flow field, respectively,

$$P = G(h-z) - s\nabla^2 h, \quad \theta = \theta_1 - \frac{B(\theta_1-\theta_2)z}{1+Bh}, \tag{11}$$

$$u = \Sigma_x Q_2(z) + z\Omega_x, \quad v = \Sigma_y Q_2(z) + z\Omega_y, \tag{12a}$$

$$w = -\tfrac{1}{2}z^2\nabla h\cdot\nabla\Sigma - Q_3(z)\nabla^2\Sigma - \tfrac{1}{2}z^2\nabla\cdot(\nabla\Omega). \tag{12b}$$

Here, the subscripts x, y denote the respective partial derivatives, $\nabla \equiv (\partial_x, \partial_y)$, $\Sigma = -Gh + s\nabla^2 h$, $Q_3(z) = \frac{1}{2}hz^2 - \frac{1}{6}z^3$, $Q_2(z) = Q_3'(z)$, $\Omega = (\theta_2 + (\theta_1-\theta_2)/(1+Bh) - \theta_0)^2$ and θ_Γ is the interface temperature given via

$$\theta_\Gamma = \theta_2 + \frac{\theta_1-\theta_2}{1+Bh}, \tag{13}$$

with $\theta_i = \theta(T = T_i)$, $i = 1, 2$, see (9b), and $\theta_0 = \theta(T = T_0)$ being the dimensionless temperature at which the surface tension obtains its minimal value. Two complementary cases will be considered:

case I: $\theta_1 = 1$, $\theta_2 = 0$ liquid heated from the bottom,

case II: $\theta_1 = 0$, $\theta_2 = 1$ liquid cooled from the bottom.

The first (second) case states that the bottom temperature is higher (lower) than that of the ambient air.

The motion in the two-dimensional liquid layer in the (x, z)-plane ($v = 0$, $\partial_y = 0$) as given by (12) can be presented in terms of the streamfunction ψ

$$\psi = s\left(\frac{hz^2}{2} - \frac{z^3}{6}\right)h_{xxx} + Bz^2\left(\delta - \frac{1}{1+Bh}\right)\frac{h_x}{(1+Bh)^2}, \tag{14}$$

with

$$\delta = \begin{cases} \theta_0, & \text{case I,} \\ 1-\theta_0, & \text{case II.} \end{cases}$$

In (11)–(14), all flow quantities are expressed in terms of dimensionless thickness of the film $h(x, t)$. The expansion yields a consistency relation for $h(x, t)$ which renders the spatiotemporal evolution of QM induced variations in film thickness that evolve according to

$$h_{\tau^*} + \nabla\cdot\left\{\left[-Gh^3 + \frac{Bh^2 D(h)}{(1+Bh)^2}\right]\nabla h\right\} + \tfrac{1}{3}s\nabla\cdot[h^3\nabla(\nabla^2 h)] = 0, \tag{15}$$

where

$$D \equiv D_{QM} = \delta - \frac{1}{1+Bh}. \tag{16a}$$

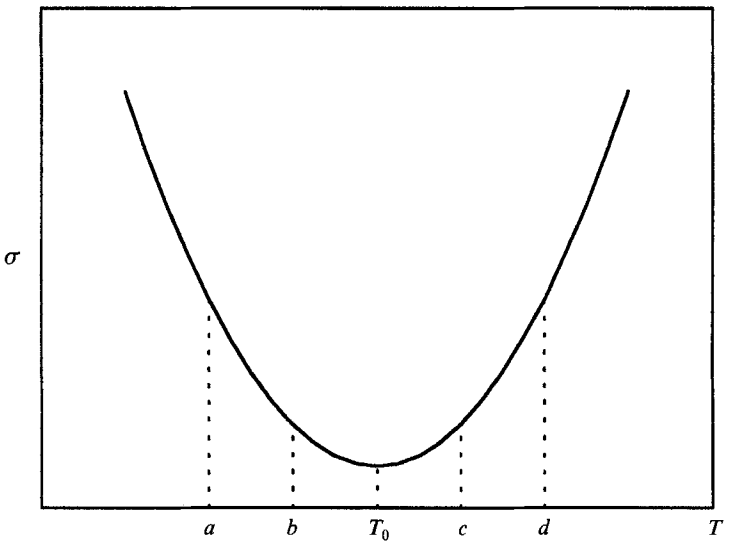

FIGURE 1. Sketch of the quadratic dependence of surface tension on temperature. The temperatures T_-, T_+ are represented respectively by the points a, b in case (a), c, d in case (b) and b, c in case (c).

Once $h(x, t)$ is determined, all other flow quantities follow directly from (11)–(14). As a consequence of the scaling (9a) the basic state is given as $h = 1$.

Note the three different domains of the parameter θ_0, shown on figure 1 relevant for the study of the QM instability:

(a) $T_- < T_+ < T_0$ then $\theta_0 > 1$,

(b) $T_0 < T_- < T_+$ then $\theta_0 < 0$,

(c) $T_- < T_0 < T_+$ then $0 < \theta_0 < 1$.

To understand the changes caused by the nonlinear dependence of surface tension on the temperature, it is imperative to compare our problem with one which is similar but in which the conventional, linear, dependence on temperature is assumed. Recently, using a similar setting, we derived such an equation which describes the evolution of a film induced by the conventional LM instability (Oron & Rosenau 1992). In form it is similar to (15) but

$$D \equiv D_{LM} = -\tfrac{1}{2}m, \quad m = \begin{cases} -1, & \text{case I,} \\ +1, & \text{case II.} \end{cases} \tag{16b}$$

In case I, (15) together with (16b) also appeared in Burelbach *et al.* 1988 (their equation (5.18)) and in Tan, Bankoff & Davis (1990) (their equation (16)). Since in both problems a different Marangoni number is used to define the characteristic velocity, it implies that the value U_0 used for normalization is different in both problems. As is typical of the asymptotic approach, the three-dimensional problem was effectively reduced to a two-dimensional problem.

Under normal conditions the effect due to gravity dominates thermocapillarity. To stress the essential differences between the linear and quadratic thermocapillarity, we focus on the weightless case and set $G \equiv 0$. It is seen from (15)–(16) that the fluid layer undergoes QM instability for $\delta > 1$ and LM instability for $m < 0$ if the periodic box is adequately large and the film thickness does not exceed a certain critical, δ-dependent value in the QM case.

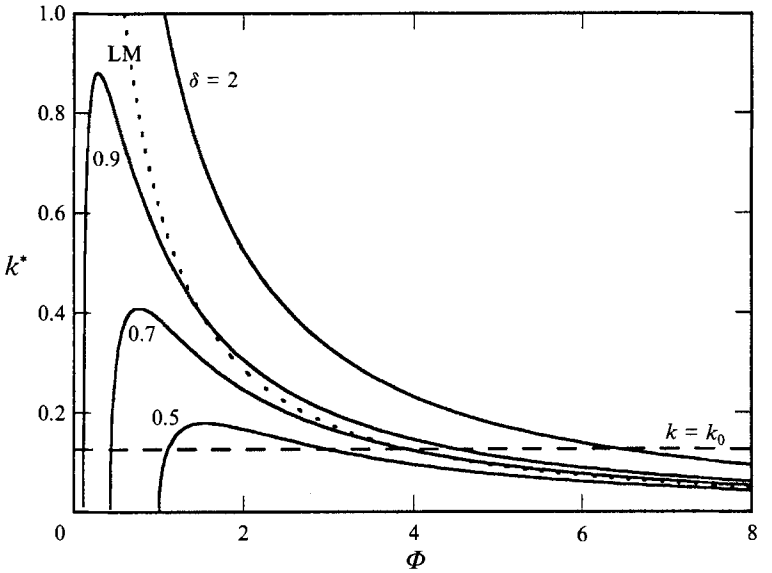

FIGURE 2. The dimensionless cutoff wavenumber k^* as a function of dimensionless film thickness Φ for the linear Marangoni (LM) and the quadratic Marangoni (QM) instabilities for various values of parameter δ. The wavenumbers of the unstable modes are located under the corresponding curve. The line $k = k_0$ shows the wavenumber of the fundamental mode which can be accommodated in a domain of size L. The value of k_0 shown corresponds to $L = 16\pi$.

The normalization $\phi = Bh$, $\tau = B\tau^*/s$, $(x, y) = (s/B^2)^{1/2}(\xi, \zeta)$ then reduces (15) and (16) into

$$\phi_\tau + \nabla\cdot\left[\frac{D\phi^2}{(1+\phi)^2}\nabla\phi\right] + \tfrac{1}{3}\nabla\cdot[\phi^3\nabla(\nabla^2\phi)] = 0, \tag{17}$$

where $D = D_{QM} = \delta - \dfrac{1}{1+\phi}$, $\nabla \equiv (\partial_\xi, \partial_\zeta)$, $0 \leqslant \xi \leqslant L_1$, $0 \leqslant \zeta \leqslant L_2$.

Introducing perturbations of the normal form, $\exp(ik_\xi\xi + ik_\zeta\zeta + \lambda\tau)$, around the uniform state, $\phi = \Phi = B > 0$ (recall that in the basic state $h = 1$, therefore $\Phi = B$), yields the dispersion relation

$$\lambda = k^2\Phi^3\left[\frac{D(\Phi)}{\Phi(1+\Phi)^2} - \tfrac{1}{3}k^2\right], \tag{18}$$

$D(\Phi)$ is either D_{QM} or D_{LM}, and $\boldsymbol{k}^2 = k_\xi^2 + k_\zeta^2$. The cutoff stability wavenumber, k^*, in both cases is given as

$$k^*_{QM} = \frac{\sqrt{3}}{\Phi^{1/2}(1+\Phi)}\left(\delta - \frac{1}{1+\Phi}\right)^{1/2}, \quad k^*_{LM} = \frac{\sqrt{3}}{(2\Phi)^{1/2}(1+\Phi)}. \tag{19}$$

The $k < k^*$ disturbances are unstable, which is typical of all longwave instabilities. Clearly, for such instability to materialize, the periodic domain must be large enough to accommodate at least the longest (the smallest k) unstable mode. Figure 2 shows the cutoff wavenumber, k^*, for the QM with several values of δ. The LM curve was calculated using (18) assuming that the size of the one-dimensional periodic domain is fixed. The value $k = k_0$ corresponds to the fundamental wave which is accommodated in the considered domain taking its size $L = 16\pi$. The unstable spectrum of the system is located under the curves shown. As it is seen from figure 2, the QM instability of a

film of a uniform thickness Φ, is triggered in the case (c), ($0 < \delta < 1$) for values of Φ which are between the two intersection points of the line $k = k_0$ with the corresponding curve. The necessary condition for QM instability follows from (19),

$$\Phi > \frac{1-\delta}{\delta}, \tag{20}$$

and does not depend on the direction of the vertical temperature gradient. This is one of the differences between the LM and QM instabilities. Recall that the LM instability arises for any film of sufficiently small thickness (Davis 1987; Oron & Rosenau 1992). It follows from (20) that the layer is stable if $\delta \to 0+$, corresponding to $T_- \uparrow T_0$ for the case I, and $T_+ \downarrow T_0$ for the case II.

If the domain size is sufficiently large it follows from (18) and figure 2 that $\delta > 1$ (cases I(a) and II(b)) implies QM instability when the thickness of the layer does not exceed a value given by the point of intersection of the line $k = k_0$ with the corresponding curve. Qualitatively these two cases resemble the conventional LM instability which occurs when the product $(T_1 - T_2)(\sigma_+ - \sigma_-)$ is negative. The latter is described by (15) and (16b). Similarly, $\delta < 0$ (cases I(b) and II(a)) implies stability of the film.

Comparing the cutoff wavenumbers in (19), we find that for $\delta < \frac{1}{2}$, $k^*_{QM} < k^*_{LM}$ for any amplitude Φ. This means that when $\delta < \frac{1}{2}$, a QM unstable state is also LM unstable. For $\delta < \frac{1}{2}$ there is also a range of Φ which is QM stable but LM unstable. This suggests a number of possible technological applications which will be discussed in §4. Now if $\delta > \frac{3}{2}$, LM instability implies QM instability for any Φ. In contradistinction to the other case, for $\delta > \frac{3}{2}$ there is a range of amplitudes Φ where the flow is QM unstable but is LM stable.

Equation (17) can be rewritten into a Cahn–Hilliard type form

$$\phi_\tau = \nabla \cdot \left[\phi^3 \nabla \left(\frac{\delta F}{\delta \phi}\right)\right], \quad F = \int_\Omega [-V(\phi) + \tfrac{1}{6}|\nabla \phi|^2]\, \mathrm{d}\Omega. \tag{21}$$

Here $V(\phi)$ is the potential energy

$$V(\phi) = (\delta - 1)\,\phi \ln \frac{\phi}{1+\phi} + \frac{\phi^2}{2(1+\phi)} - A\phi, \tag{22}$$

Ω is a either unbounded or a periodic domain and A is a constant of integration. Note that F is a decreasing function along any trajectory:

$$\frac{\mathrm{d}F}{\mathrm{d}\tau} = -\int_\Omega \phi^3 \left| \nabla \left(\frac{\mathrm{d}V}{\mathrm{d}\phi} + \tfrac{1}{3}\nabla^2 \phi\right)\right|^2 \mathrm{d}\Omega \leqslant 0, \tag{23}$$

therefore F is a Lyapunov functional for (21). Steady states of the system, therefore, if exist, are solutions of the equation

$$\nabla^2 \phi + 3\frac{\mathrm{d}V}{\mathrm{d}\phi} = \text{const},$$

and in the one-dimensional case the latter can be recast into

$$\phi_\xi^2 + V(\phi) = \text{const}.$$

We have to comment on the presence of an integration constant A in the potential energy (22). A typical potential energy is usually at least a quadratic function in ϕ for large arguments, and addition of a linear part amounts only to shift in the frame of reference. However, in the present problem without A, the potential energy becomes

linear for large argument and thus deformable under linear shifts. Indeed taking $A > \frac{1}{2}$ deforms the asymptotic behaviour of the original potential energy. The new potential energy generates a new class of equilibria.

Similar results were obtained in the LM case (Oron & Rosenau 1992; Deissler & Oron 1992) for the potential $V(\phi)$ given as

$$V(\phi) = \tfrac{1}{2}\phi \ln \frac{\phi}{1+\phi} - A\phi + \gamma\phi^2, \tag{24}$$

where γ is a gravity parameter.

We recall that if a system has a Lyapunov functional bounded from below (a free energy functional decreasing along all trajectories) any initial data evolves into a steady state. We focus here on the existence of continuous steady periodic (CSP) states, i.e. states with non-vanishing amplitude everywhere. The CSP states are admissible if both of the following conditions are met: (*a*) the potential energy, $V(\phi)$, associated with the Lyapunov functional is bounded from above; (*b*) there exists a local minimum of the potential energy at $\phi \neq 0$. Figure 3 displays the admissible curves of the potential energy, $V(\phi)$, (see (22)). Our studies show that the conditions (*a*), (*b*) are satisfied simultaneously if $0 < \delta < 1$ and $f(\delta) < A < \frac{1}{2}$, $f(\delta)$ being a function of δ, see curves 3, 4 corresponding to $A = 0.48, 0.49$, respectively. CSP states exist in the valleys of these curves (marked by the dashed lines). These potential energy curves qualitatively resemble those found for films flowing under the influence of both destabilizing gravity and LM-thermocapillarity (Oron & Rosenau 1992; Deissler & Oron 1992). Curves 1, 2, 5, 6 of figure 3 do not satisfy one of the conditions (*a*), (*b*) and therefore the existence of CSP states is not assured. A similar situation is found also for the LM case without gravity. Our numerical studies of this case (Oron & Rosenau 1992) revealed that the evolution of small-amplitude initial data lead ultimately to the rupture of the film, thus the CSP states do not exist. This conclusion holds also for the QM case with $|\delta| > 1$. We emphasize that if condition (*b*) is not met, then the potential energy attains its minimal value at zero, $\phi = 0$. This in turn implies that periodic steady states if they exist are not continuous, i.e. they are ruptured.

As we have seen in figure 3 the topological structure of the potential energy curves, and therefore the existence of the CSP states, depends on the values of δ and A. The parameter δ is defined through relevant temperatures and thus may be viewed as a control parameter. However, the value of A reflects, among other things, the impact of boundary conditions on the dynamics and in general cannot be predetermined. The choice of various values of A in figure 3 is intended to show the main possible topological structures of the potential energy, without stating how such effective potentials can be materialized. Therefore, the quest for non-ruptured steady states, living in the valleys of the potential energy, can, at least at this stage of our understanding, be resolved only by relying on the results of numerical experiments.

Conservation laws

A: the total mass of the film is conserved

$$\frac{\mathrm{d}}{\mathrm{d}\tau}\int_\Omega \phi \,\mathrm{d}\Omega = 0. \tag{25}$$

B: multiply (17) by ϕ^{-2} and integrate over Ω with periodic boundary conditions to obtain

$$\frac{\mathrm{d}}{\mathrm{d}\tau}\int_\Omega \frac{\mathrm{d}\Omega}{\phi} = 2\int_\Omega \left[\frac{D(\phi)}{\phi(1+\phi)^2}|\nabla\phi|^2 - \tfrac{1}{3}|\nabla^2\phi|^2\right]\mathrm{d}\Omega. \tag{26}$$

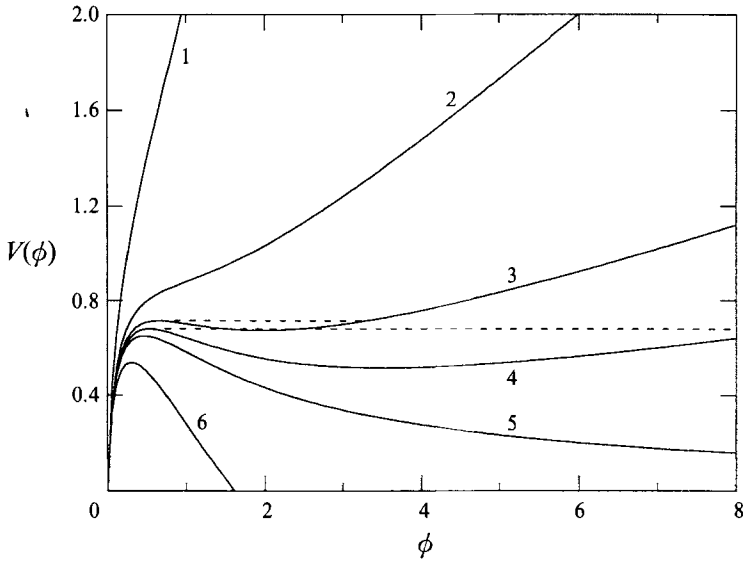

FIGURE 3. The potential energy $V(\phi)$ for $\delta = 0.5$ and various values of A: $1-A = 0.25$, $2-A = 0.45$, $3-A = 0.48$, $4-A = 0.49$, $5-A = 0.5$, $6-A = 0.55$. Steady states reside in the valleys of the potential energy curves designated by the dashed lines.

3. Numerical studies

Our numerical efforts focused on the one-dimensional version of (17) which describes a two-dimensional flow, namely

$$\phi_\tau + \frac{\partial}{\partial\xi}\left[\frac{\phi^2}{(1+\phi)^2}\left(\delta - \frac{1}{1+\phi}\right)\phi_\xi\right] + \frac{1}{3}\frac{\partial}{\partial\xi}[\phi^3\phi_{\xi\xi\xi}] = 0. \tag{27}$$

Equation (27) was solved numerically in a periodic domain $0 \leqslant \xi \leqslant L$. We used periodic boundary conditions and the initial condition

$$\phi_0(\xi) = \Phi + \vartheta \sin(2\pi\xi/L) \quad \text{with} \quad \vartheta \ll 1.$$

Note that the two-dimensional flow described by (27) is the least stable among general three-dimensional configurations. This property is typical for long-wave instability phenomena: in three dimensions, the presence of the k_ζ-component of the wavevector $\boldsymbol{k}$ increases the magnitude of k and thus narrows the unstable band. A similar effect can be achieved through the reduction of the size of the transverse periodic box.

The emerging solutions whether linearly stable or not, appear always to be globally bounded. Globally unbounded solutions do not arise. This is consistent with a conjecture stated for a generalized Cahn–Hilliard equation (Hocherman & Rosenau 1993) of the form:

$$\phi_\tau = \frac{\partial}{\partial\xi}\left\{M(\phi)\frac{\partial}{\partial\xi}[Q(\phi) - R(\phi)\phi_{\xi\xi}]\right\}, \tag{28}$$

namely, if $\lim_{s\to\infty}|Q(s)/sR(s)| = 0$, then the solutions of (28) with reasonable boundary conditions are globally bounded. With $M(\phi) = \phi^3$ and $R(\phi) = \frac{1}{3}$ we see that (27) becomes a particular case of (28) if we take

$$Q(\phi) = -\frac{\mathrm{d}V(\phi)}{\mathrm{d}\phi} = -(\delta-1)\left[\ln\frac{\phi}{1+\phi} + \frac{1}{1+\phi}\right] + \frac{1}{2(1+\phi)^2} + A. \tag{29}$$

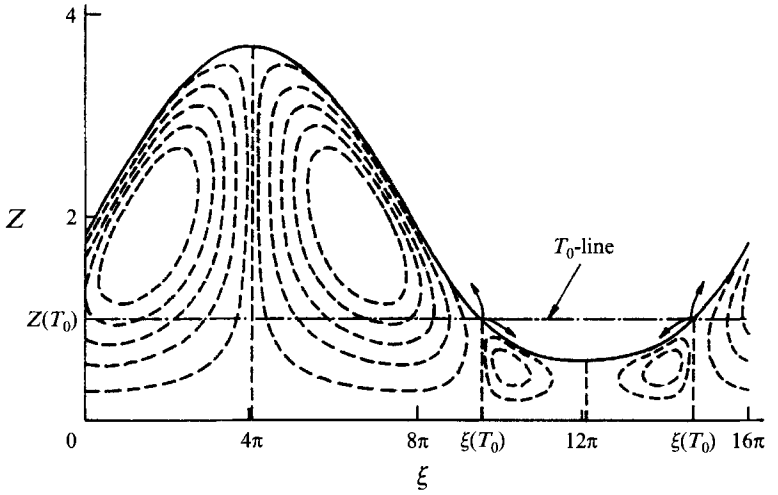

FIGURE 4. The interfacial shape (time $\tau = 40000$) shown here evolved from initial perturbation of the uniform state $\Phi = 2$, $\vartheta = 0.01$ for $\delta = 0.5$, $L = 16\pi$. This shape is very close to the terminal stable steady state solution of (27) for the quadratic Marangoni (QM). Streamlines of the flow field (dashed lines) are calculated via (30). The periodic domain shown consists of four convective cells contained between the extremal points of the interface and the $\xi(T_0)$ points which are points of the minimal surface tension at $T = T_0$. The arrows indicate the direction of the flow at $\xi(T_0)$ which are stagnation points.

A detailed numerical study of (27) is not intended in the present paper. We note, however, that the few tens of numerical experiments with a fixed $L = 16\pi$, show that beside a rupture of the film into separate drops caused by a small perturbation of the film, steady states may emerge after a long evolution. In our numerical study, steady states were found for $\delta \leqslant 0.5$ (see figure 4). Figure 4 displays the steady interfacial shape which results from the evolution due to the QM instability. Here $\delta = 0.5$, $\vartheta = 0.01$, $\Phi = 2$ and $L = 16\pi$. For $\delta \geqslant 0.6$ a film rupture similar to the one emerging in the conventional LM flow arises (see figure 5).

To elucidate the qualitative difference in interfacial patterns which may arise owing to the QM and LM instabilities, we followed the spatiotemporal behaviour of the liquid film of a given thickness at temperatures of $T_1 = 45$ °C, $T_2 = 35$ °C when the fluid is alternatively pure water (undergoing the LM instability) and a dilute aqueous solution of *n*-heptanol (undergoing the QM instability), both in contact with air at their free surface. In order to calculate the dimensionless parameters governing the evolution of the film we use the following physical data for the substances of interest: for a pure water: $\alpha_L = 0.15 \times 10^{-3}$ N (mK)$^{-1}$, $\sigma_0 = 69.5 \times 10^{-3}$ N m^{-1}. For an aqueous solution of *n*-heptanol (Legros *et al.* 1984): $\alpha_Q = 4.4 \times 10^{-6}$ N m^{-1} K^{-2}, $\sigma_0 = 3.53 \times 10^{-2}$ N m^{-1}, $T_0 = 40$ °C. The physical properties of the bulk are only slightly modified by small quantities of the solute (Legros *et al.* 1984) and the main changes are limited to the interfacial properties. We also assume that the values of the Biot number are identical in both cases. The corresponding values of the relevant parameters are: for the LM case (water) $U_0 \approx 1.50$ m s^{-1}, $S \approx 46.33$, while for the QM case (water with *n*-heptanol) $U_0 \approx 0.22$ m s^{-1}, $S \approx 16.05$, $\delta = 0.5$. (Recall that the difference in U_0 is due to the different Marangoni numbers used to define U_0.) The rescaled sizes of the periodic domain in both cases are taken as $L = 9.416\pi$ and $L = 16\pi$ for the LM and QM, respectively, both corresponding to the specified physical size of the periodic box $La\,S^{1/2}/B$. (The domain size $L = 16\pi$ for the QM case is close to the fastest wavelength.

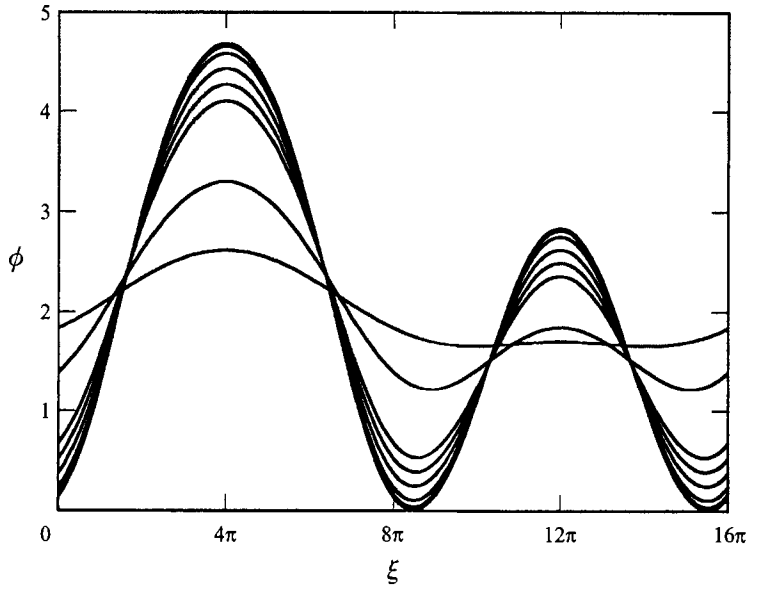

FIGURE 5. Spatiotemporal evolution of the interface toward rupture of the film as predicted by (27) for the quadratic Marangoni (QM) instability with $\delta = 0.9$, $L = 16\pi$, $\Phi = 2$ and $\vartheta = 0.01$, $\tau = 1600$.

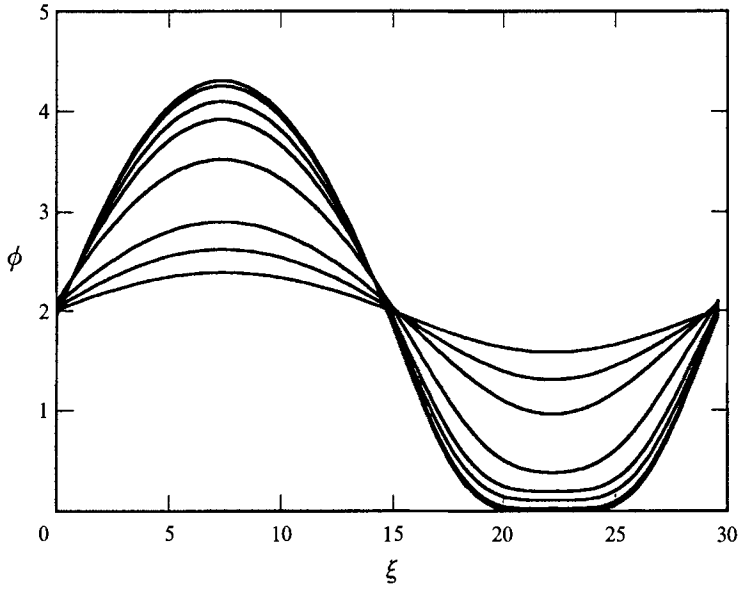

FIGURE 6. Spatiotemporal evolution of the interface toward rupture of the film owing to the linear Marangoni (LM) (equations (17), (16*b*)) with $L = 9.416\pi$, $\Phi = 2$, $m = -1$ and $\vartheta = 0.01$.

For the LM, the properly rescaled value is $L = 9.416\pi$. The rescaled dimensionless thickness of the film is assumed to be $\Phi = 2$. The evolutions of the QM and LM instabilities are shown in figures 4 and 6, respectively. The QM leads to a stable steady state which preserves the continuity of the film, but the LM results in a rupture of the film.

In the absence of gravity the LM instability always causes the film to rupture. This is consistent with a criterion (Tan *et al.* 1990), according to which continuous steady

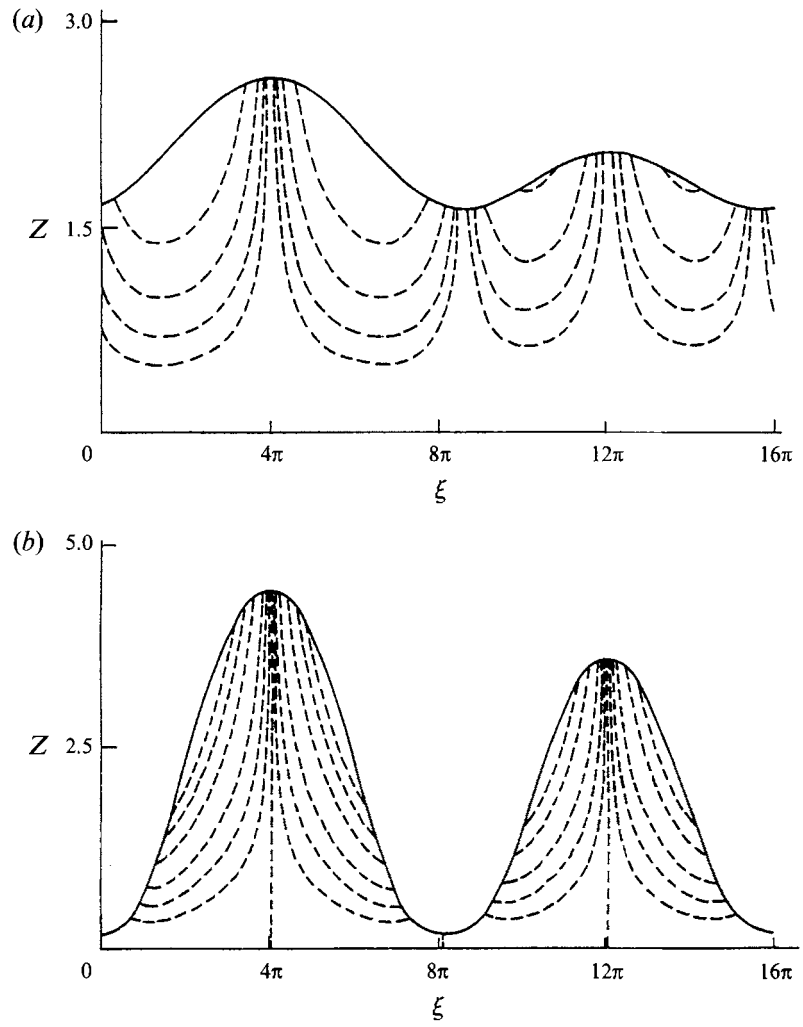

FIGURE 7. Typical flow field for transient states in the LM and QM (either to case (*a*) or (*b*), $|\delta| > 1$) induced flows. The flow is directed from the thinner part of the film to the thicker one and this leads to amplification of the perturbations and to the rupture of the film. The graphs shown (the dashed lines are streamlines) are obtained for the QM instability with $\delta = 1.25$, $\Phi = 2$, $\vartheta = 0.01$ and $L = 16\pi$. (*a*) $\tau = 590$, (*b*) $\tau = 730$.

profiles of a liquid layer can be sustained when a parameter inversely proportional to the acceleration due to gravity g is smaller than a certain critical value. In the absence of gravity that parameter is always infinite, and therefore the film ruptures.

Streamlines of the steady flow were calculated for $\delta = 0.5$ and are displayed in figure 4. In expression (14) for the rescaled stream function we eliminate using (27) the third derivative $\phi_{\xi\xi\xi}$. Thus

$$\psi = -\frac{B\phi_\xi Z^2}{2(1+\phi)^2}\left(\delta - \frac{1}{1+\phi}\right)\left(1-\frac{Z}{\phi}\right), \tag{30}$$

where $Z = Bz$. It is clear that the convective cells are constrained between the surfaces $Z = 0$, $Z = \phi$, and vertical planes corresponding to the extrema of the interface and to the points at the interface where $\phi = (1-\delta)/\delta$. The number of convective cells within the periodic domain is four times the number of humps of the steady interfacial

pattern. This feature of the QM induced flow differs from the LM flow whenever the former admits a steady state (e.g. when the bottom temperature varies periodically (Tan *et al.* 1990)). The complexity of the QM induced pattern is due to the non-monotone behaviour of surface tension. Specifically, in QM flow the location of stagnation points usually differs from the location of the extremal points of the interface. On the interface of $Z = Z(T_0)$ lines (corresponding to $\phi = (1-\delta)/\delta$), the surface tension is minimal, the surface shear stresses (proportional to the gradient of surface tension on the surface) are directed outward, and induce the flow as shown in figure 4. The flow is descending in extremal locations of the interface. It is also found that in the convective cells adjacent to the minimal point, the flow is much slower than those related to the maximal one.

Figure 7 shows temporal snapshots of the evolution of the flow field with the streamlines and the film interface displayed. Those are typical for the LM and QM induced flows when the latter belongs to a monotone branch of the surface tension curve $\sigma(T)$, $|\delta| > 1$. Note that these flows do not settle into a steady state and, as follows from the kinematic condition, equation (8), the free surface is not a streamline. The liquid flows from the thinner part of the film into the thicker one and this necessarily leads to amplification of the perturbations and to the rupture of the film.

4. Summary and concluding remarks

We have studied the evolution of a thin liquid film due to quadratic Marangoni instability found in dilute aqueous alcohol solutions. Exploiting the thinness of the film with respect to the characteristic length of perturbations, we derive equation (15) which describes the interfacial evolution of the film. Similarly to the conventional linear Marangoni effect, the quadratic Marangoni (QM) effect plays an important role in microgravity conditions. Therefore, to stress the differences between these flows we consider the quadratic Marangoni effect in the absence of gravity.

Not surprisingly, a novel modus operandi is found when the temperature range of the film centres around the temperature corresponding to a dip in surface tension. While in the conventional case the theory predicts that the film will always rupture, here we find stable steady states with perfectly continuous interfaces evolving out of arbitrary small initial perturbations of the interface. When the temperature range of the film is wholly contained in either of the monotone parts of the $\sigma(T)$ (surface-tension–temperature) curve, the emerging patterns tend to be qualitatively similar to those observed in the conventional, linear, Marangoni case. In particular, in this regime we do observe the formation of separate drops. Naturally, QM induced flows have a different stability threshold, there are cases where LM stability (instability) implies a QM stability (instability) or vice versa, as well as regimes in which one case is only in part embedded in the other. For more details see §3.

An interesting potential application comes about as follows: since in dilute aqueous solution of long-chain alcohol only surface tension has changed without affecting other bulk properties of the fluid, one can consider tailoring a desirable $\sigma(T)$ dependence with a particular application (i.e. coating, crystal growth, etc.) in mind wherein particular patterns will be induced or precluded. This will be achieved by centring the surface tension minimum at a desirable location with respect to the temperature range of the film.

We acknowledge the support by the Technion VPR – Posnansky Research Fund in High Temperature. A.O. acknowledges the support by the Technion VPR –

Israel–Mexico Energy Research Fund and the Fund for promotion of research in Technion. The work of P. R. was also supported in part by the AFOSR Grant F49620-92-J0054.

REFERENCES

BURELBACH, J. P., BANKOFF, S. G. & DAVIS, S. H. 1988 Nonlinear stability of evaporating/condensing liquid films. *J. Fluid Mech.* **195**, 463–494.

CLOOT, A. & LEBON, G. 1986 Marangoni convection induced by a nonlinear temperature-dependent surface tension. *J. Phys. Paris* **47**, 23–29.

DAVIS, S. H. 1987 Thermocapillary instabilities. *Ann. Rev. Fluid Mech.* **19**, 403–435 and references therein.

DEISSLER, R. J. & ORON, A. 1992 Stable localized patterns in thin liquid films. *Phys. Rev. Lett.* **68**, 2948–2951.

GUPALO, YU. P. & RYAZANTSEV, YU. S. 1989 Thermocapillary motion of a liquid with a free surface with nonlinear dependence of the surface tension on the temperature. *Fluid Dyn.* **23**, 752–757.

GUPALO, YU. P., RYAZANTSEV, YU. S. & SKVORTSOVA, A. V. 1990 Effect of thermocapillary forces on free-surface fluid motion. *Fluid Dyn.* **24**, 657–661.

GUYON, E. & PANTALONI, J. 1980 Effet de tension superficielle sur la convection de Rayleigh–Bénard. *CR Acad. Sci. Paris* B **290**, 301–304.

HOCHERMAN, T. & ROSENAU, P. 1993 On KS-type equations describing the evolution and rupture of a liquid interface. *Physica* D, **67**, 113–125.

LEGROS, J. C. 1986 Problems related to non-linear variations of surface tension. *Acta Astr.* **13**, 697–703.

LEGROS, J. C., LIMBOURG-FONTAINE, M. C. & PETRE, G. 1984 Influence of a surface tension minimum as a function of temperature on the Marangoni convection. *Acta Astr.* **11**, 143–147.

LIMBOURG, M. C. & GEORIS, PH. 1989 Preliminary results of Texus 19 (Temo6-8) experiment: Marangoni convection around a surface tension minimum. *Proc. VIIth Eur. Symp. on Materials and Fluid Sci. in Microgravity (Oxford, UK)*, ESA SP-295, pp. 347–351.

ORON, A. & ROSENAU, P. 1992 Formation of patterns induced by thermocapillarity and gravity. *J. Phys. France* II **2**, 131–148.

PEARSON, J. R. A. 1958 On convection cells induced by surface tension. *J. Fluid Mech.* **4**, 489–500.

TAN, M. J., BANKOFF, S. G. & DAVIS, S. H. 1990 Steady thermocapillary flows of thin liquid layers. I. Theory. *Phys. Fluids* A **2**, 313–321.